


# Synaptic plasticity of inhibitory synapses onto medial olivocochlear efferent neurons

Lester Torres Cadenas<sup>1</sup>, Hui Cheng<sup>2</sup> and Catherine J. C. Weisz<sup>1</sup> 

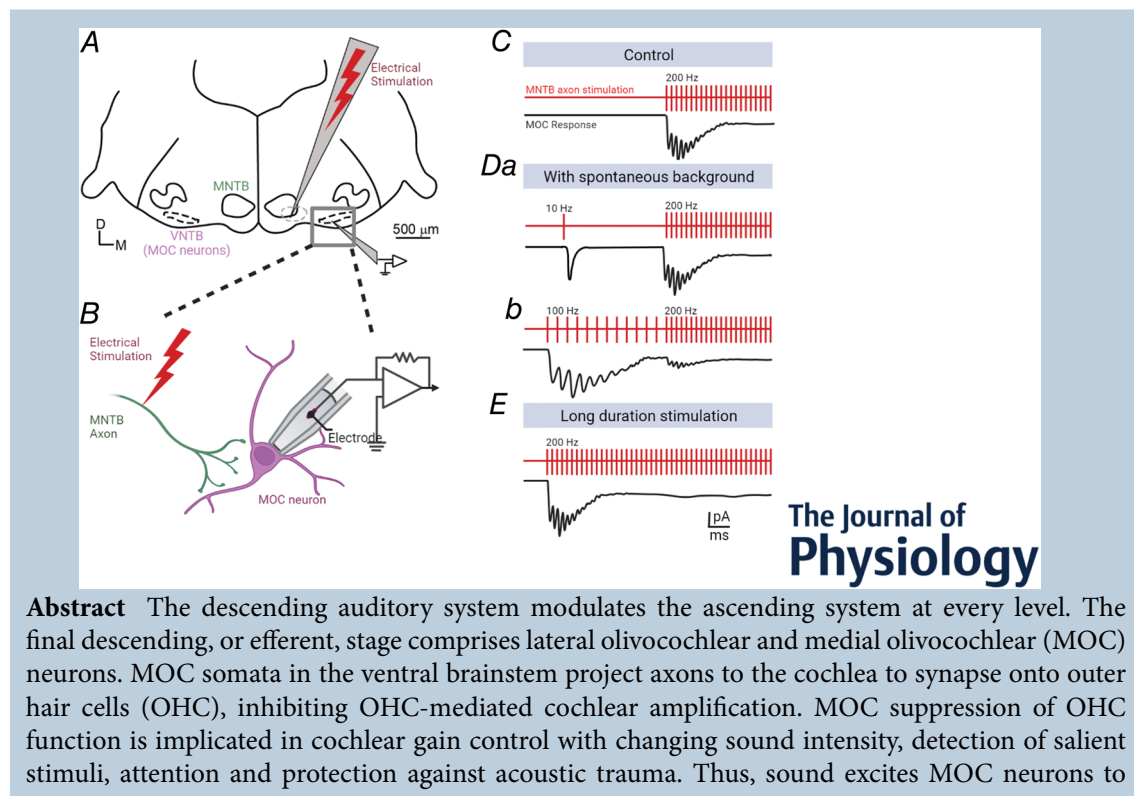
<sup>1</sup>Section on Neuronal Circuitry, National Institute on Deafness and Other Communication Disorders, NIH, Bethesda, MD, USA

<sup>2</sup>Bioinformatics and Biostatistics Collaboration Core, National Institute on Deafness and Other Communication Disorders, NIH, Bethesda, MD, USA

Edited by: Ian Forsythe & Conny Kopp-Scheinflug

Linked articles: This article is highlighted in a Perspective article by Kuenzel. To read this article, visit <https://doi.org/10.1113/JP283180>.

The peer review history is available in the Supporting information section of this article (<https://doi.org/10.1113/JP282815#support-information-section>).



**Lester Torres Cadenas** was born and raised in Cuba. He earned his bachelor's degree in Biology in 2003 and his master's degree in Biology in 2008 at the University of Havana. He arrived in the United States in 2012 and became Lab Manager for Dr Maria (Lania) Rubio in the Otolaryngology Department at the University of Pittsburgh. He is currently Lab Manager in the lab of Dr Catherine Weisz at the NIH/NIDCD in Bethesda, MD. He was integral to setting up the lab when it was established in 2015, and it has become his second home.



This article was first published as a preprint. Cadenas LT, Cheng H & Weisz CJC (2022). Synaptic plasticity of inhibitory synapses onto medial olivocochlear efferent neurons. *bioRxiv*. <https://doi.org/10.1101/2022.01.05.475100>.

Published 2022. This article is a U.S. Government work and is in the public domain in the USA. The Journal of Physiology published by John Wiley & Sons Ltd on behalf of The Physiological Society.

DOI: 10.1113/JP282815

This is an open access article under the terms of the Creative Commons Attribution-NonCommercial-NoDerivs License, which permits use and distribution in any medium, provided the original work is properly cited, the use is non-commercial and no modifications or adaptations are made.

provide negative feedback of the cochlea. Sound also inhibits MOC neurons via medial nucleus of the trapezoid body (MNTB) neurons. However, MNTB–MOC synapses exhibit short-term depression, suggesting reduced MNTB–MOC inhibition during sustained stimuli. Further, due to high rates of both baseline and sound-evoked activity in MNTB neurons *in vivo*, MNTB–MOC synapses may be tonically depressed. To probe this, we characterized short-term plasticity of MNTB–MOC synapses in mouse brain slices. We mimicked *in vivo*-like temperature and extracellular calcium conditions, and *in vivo*-like activity patterns of fast synaptic activation rates, sustained activation and prior tonic activity. Synaptic depression was sensitive to extracellular calcium concentration and temperature. During rapid MNTB axon stimulation, postsynaptic currents in MOC neurons summated but with concurrent depression, resulting in smaller, sustained currents, suggesting tonic inhibition of MOC neurons during rapid circuit activity. Low levels of baseline MNTB activity did not significantly reduce responses to subsequent rapid activity that mimics sound stimulation, indicating that, *in vivo*, MNTB inhibition of MOC neurons persists despite tonic synaptic depression.

(Received 7 January 2022; accepted after revision 4 April 2022; first published online 20 April 2022)

**Corresponding author** C. J. C. Weisz: Section on Neuronal Circuitry, National Institutes of Health, National Institute on Deafness and Other Communication Disorders, Bethesda, MD 20892, USA. Email: catherine.weisz@nih.gov

**Abstract figure legend** Characterization of synaptic plasticity of inhibitory synapses in brainstem slices. *A*, schematic representation of experimental procedure. In brainstem slices, whole-cell patch-clamp recordings are performed from identified medial olivocochlear (MOC) neurons. Electrical stimulation of medial nucleus of the trapezoid body (MNTB) axons evokes neurotransmitter release onto MOC neurons, which are recorded as evoked postsynaptic currents (ePSC) in the MOC neuron. *B*, schematic representation of an MNTB axon (green) forming synapses onto an MOC neuron (purple). Axon stimulation indicated in red; patch-clamp electrode indicated. *C–E*, schematized results from experiments in which trains of electrical stimulation are applied to MNTB axons (red) resulting in ePSCs in MOC neurons (black). Note that PSCs are not to scale. *C*, fast (200 Hz) MNTB axon stimulation evokes PSCs that summate and undergo short-term synaptic depression. *Da*, following a low (10 Hz) rate of background MNTB axon stimulation, fast (200 Hz) axon stimulation evokes PSCs equivalent in amplitude to those evoked in control conditions. *Db*, following a high (100 Hz) rate of background MNTB axon stimulation, subsequent fast stimulation (200 Hz) evokes PSCs that are significantly reduced in amplitude compared to control. *E*, long duration application of fast (200 Hz) trains of electrical stimulation to MNTB axons evokes PSCs in MOC neurons that summate to a peak ePSC, followed by synaptic depression that reduces the amplitude of the response to a tonic level of inhibition. *B–E* generated in BioRender; all panels assembled in BioRender (biorender.com).

### Key points

- Inhibitory synapses from the medial nucleus of the trapezoid body (MNTB) onto medial olivocochlear (MOC) neurons exhibit short-term plasticity that is sensitive to calcium and temperature, with enhanced synaptic depression occurring at higher calcium concentrations and at room temperature.
- High rates of background synaptic activity that mimic the upper limits of spontaneous MNTB activity cause tonic synaptic depression of MNTB–MOC synapses that limits further synaptic inhibition.
- High rates of activity at MNTB–MOC synapses cause synaptic summation with concurrent depression to yield a response with an initial large amplitude that decays to a tonic inhibition.

### Introduction

Mammalian auditory systems encode acoustic stimuli that occur over many orders of magnitude of sound intensity. Animals require mechanisms to shift the gain of the auditory system between softer and louder sounds both to enable soft sound detection and to prevent system saturation during loud sounds. The

medial olivocochlear (MOC) neurons are one of multiple gain control systems that adjust auditory sensitivity (Desmedt, 1962; Galambos, 1956; Geisler, 1974; Guinan & Gifford, 1988; Wiederhold & Kiang, 1970; Wiederhold & Peake, 1966). MOC neuron somata are located in the ventral brainstem, and their axons project to the cochlea to form cholinergic synapses onto outer hair cells (OHC) (reviewed in Guinan, 1996). Through coupling of

cholinergic responses in the OHC to SK or BK potassium channels, OHCs are inhibited by MOC activity (reviewed in Fuchs & Lauer, 2019). This inhibition reduces OHC activity, suppressing active processes in the organ of Corti and in turn, reducing auditory nerve activity with broadened tuning curves (Art et al., 1985; Fex, 1962a; Galambos, 1956; Mountain, 1980; Siegel & Kim, 1982; Wiederhold & Kiang, 1970). Thus, the MOC system is implicated in cochlear gain control, as well as detection of salient sounds, protection from noise trauma and auditory attention (Boero et al., 2018; Delano et al., 2007; Glenn & Oatman, 1977; Kawase et al., 1993; Maison et al., 2013; Oatman, 1976; Rajan, 1988, 1995; Reiter & Liberman, 1995; Taranda et al., 2009; Terreros et al., 2016; Tong et al., 2013; Winslow & Sachs, 1987) via their actions on OHCs.

The patterns of activity of MOC synapses onto OHCs in the cochlea are governed by MOC somatic activity, which is in turn determined by interplay between intrinsic electrical neuronal properties and synaptic inputs that provide information about sound stimuli. *In vivo* recordings from MOC axons demonstrate low sound thresholds, narrow, V-shaped tuning curves qualitatively similar to auditory nerve tuning curves, and short-latency responses to loud sounds (Brown, 1989; Fex, 1962b; Maison et al., 2003; Robertson, 1984; Robertson & Gummer, 1985). Many MOC neurons have zero to low rates of action potentials *in vivo* in the absence of sound (Brown, 1989; Maison et al., 2003; Robertson & Gummer, 1985). The presynaptic circuitry driving MOC neuron activity is incompletely known, but anatomical (Brown et al., 2003, 2013; Darrow et al., 2012; De Venecia et al., 2005) and recent functional (Romero & Trussell, 2021) work indicates that T-stellate cells of the ventral cochlear nucleus (VCN) are the primary sound-driven inputs to MOC neurons, with contributions from cells of the cochlear nucleus (CN) small shell cap (Hockley et al., 2022). MOC neurons are also strongly excited by descending projections from the inferior colliculus (IC) (Romero & Trussell, 2021). In contrast to these excitatory synaptic inputs, we previously demonstrated that MOC neurons receive inhibitory synaptic inputs from neurons of the medial nucleus of the trapezoid body (MNTB), which can suppress spontaneous action potentials in MOC neurons in brain slice preparations *in vitro* (Torres Cadenas et al., 2020). MOC neurons may also receive additional synaptic inputs from brain regions involved in sound perception, as well as those involved in other roles such as attention (Brown et al., 2013; Caicedo & Herbert, 1993; Christian Brown et al., 2013; Faye-Lund, 1986; Gómez-Nieto, Horta-Junior et al., 2008; Groff & Liberman, 2003; Horvath et al., 2003; Mulders & Robertson, 2002; Mulders et al., 2002; Ota et al., 2004; Suthakar & Ryugo, 2017; Thompson & Thompson, 1993; Vetter et al., 1993). How these various synaptic inputs integrate and impact MOC neuron activity remains an

important unanswered question in auditory processing and cochlear gain control.

MNTB neurons are an integral component of auditory brainstem circuitry, forming inhibitory synapses onto not only MOC neurons in the ventral nucleus of the trapezoid body (VNTB), but also onto other neurons of the superior olivary complex (SOC) including lateral superior olive, medial superior olive (MSO), nuclei of the lateral lemniscus and the superior peri-olivary nucleus (Banks & Smith, 1992; Glendenning et al., 1981; Kuwabara & Zook, 1991; Kuwabara & Zook, 1992; Smith et al., 1998). MNTB neurons are strongly activated by VCN globular bushy cells (GBC) which synapse onto the MNTB somata with the large calyx of Held axon terminal (Friauf & Ostwald, 1988; Held, 1893; Kuwabara et al., 1991; Ramón y Cajal, 1909; Smith et al., 1991; Spirou et al., 1990) to form a well-characterized high-fidelity synapse (Barnes-Davies & Forsythe, 1995; Borst et al., 1995; Guinan & Li, 1990; Taschenberger & von Gersdorff, 2000; Wu & Kelly, 1993; but see Kopp-Scheinpflug et al., 2003). *In vivo*, MNTB neurons have baseline spiking activity in the absence of sound that has been measured from 0.15 to 190 Hz, with averages around 10–20 Hz (Hermann et al., 2007; Kadner & Berrebi, 2008; Kopp-Scheinpflug et al., 2003; Smith et al., 1998; Sommer et al., 1993). MNTB neuron responses to sound onset exhibit a ‘primary-like with notch’ pattern peri-stimulus time histogram (Guinan & Li, 1990; Kopp-Scheinpflug et al., 2008; Paolini et al., 2001; Smith et al., 1998; Tolnai et al., 2009). MNTB neuron sound-evoked spike rates can reach to the hundreds of hertz (Kopp-Scheinpflug et al., 2008). How this fast spike rate of MNTB neurons inhibits MOC neurons to shape auditory processing is unclear.

To increase our understanding of how MOC neurons adjust their activity over the course of auditory stimuli, we characterized the short-term plasticity of the MNTB–MOC synapse. We show that short-term plasticity is affected by temperature, specifically that synaptic depression is reduced at physiological temperature. We also demonstrate that extracellular calcium concentrations that are known to modulate presynaptic neurotransmitter release affect plasticity at this synapse. MNTB–MOC synapses exhibit depression at both physiological and high extracellular calcium concentrations, and exhibit facilitation at low extracellular calcium concentrations. By applying low rates of stimulation of MNTB axons to mimic baseline spontaneous *in vivo* activity we examine the subsequent MOC synaptic responses to higher rates of activity, such as might occur at sound onset. Stimulation of MNTB–MOC synapses at typical baseline spontaneous rates does not appreciably alter subsequent synaptic activity. Importantly, we show that stimulation of the MNTB–MOC synapse at higher rates of activity significantly reduces the subsequent effect of MNTB–MOC synapses due to synaptic depression.

Finally, we test the response of MNTB–MOC synapses to long, fast stimulation to maximally depress the synapses. From this we demonstrate that MNTB neurons can maintain sustained inhibition of MOC neurons even during highly active periods. This sustained inhibition ultimately summates to reach a steady state to generate a tonic inhibition of MOC neurons.

## Methods

### Ethical approval

Animal procedures followed National Institutes of Health guidelines, as approved by the National Institute of Neurological Disorders and Stroke/National Institute on Deafness and Other Communication Disorders Animal Care and Use Committee. Male ( $n = 46$ ) and female ( $n = 39$ ) experimental mice were generated from a cross between ChAT-IRES-Cre transgenic mice on a C57BL/6J background strain (The Jackson Laboratory, Bar Harbor, ME, USA, cat. no. 028861) and tdTomato reporter mice (Ai14, The Jackson Laboratory, cat. no. 007914). Mice were housed on a 12/12 h light–dark cycle, with continuous availability of food and water. Data include recordings from 99 neurons in 92 brain slices from 85 animals. Mice were euthanized by carbon dioxide inhalation at a rate of 20% of chamber volume per minute, then decapitated.

### Animals and slice preparation

Brain slices were prepared from post-natal day (P) 14–23 mice of either sex resulting from a cross between ChAT-IRES-Cre transgenic mice on a C57BL/6J background strain (The Jackson Laboratory, cat. no. 028861), with tdTomato reporter mice (Ai14, The Jackson Laboratory, cat. no. 007914). Hemizygotes were used to prevent deleterious effects noted in ChAT-IRES-Cre homozygotes (Chen et al., 2018). As noted in the mouse line descriptions, this ChAT-IRES-Cre strain is occasionally prone to ectopic expression of Cre in vasculature, glia or non-cholinergic neurons due to the presence of the neo cassette, causing tdTomato labelling in non-cholinergic cells. If any ectopic expression patterns were observed, the tissue from the animal was not used. Following euthanasia, the brain was removed in cold artificial cerebrospinal fluid (aCSF) containing (in mM): 124 NaCl, 1.2 CaCl<sub>2</sub>, 1.3 MgSO<sub>4</sub>, 5 KCl, 26 NaHCO<sub>3</sub>, 1.25 KH<sub>2</sub>PO<sub>4</sub>, 10 dextrose. One millimolar kynurenic acid was included during slice preparation. The pH was equal to 7.4 when bubbled with 95% O<sub>2</sub>–5% CO<sub>2</sub>. Three hundred micrometre coronal brain slices containing nuclei of the SOC including the MNTB and VNTB were cut with a vibrating-blade microtome (Leica Biosystems,

Wetzlar, Germany, VT1200S) in cold aCSF. The slices were stored in a custom interface chamber at 32°C for 1 h and then allowed to cool to room temperature for electrophysiological recordings. The slices were used within 4 h of preparation.

### Patch-clamp electrophysiological recordings

Brain slices were transferred to a recording chamber continuously perfused at a rate of ~2–3 ml/min with aCSF bubbled with 95% O<sub>2</sub>–5% CO<sub>2</sub>. The majority of voltage-clamp recordings were performed at physiological temperature ( $35 \pm 1^\circ\text{C}$ ), although some were performed at room temperature ( $24 \pm 1^\circ\text{C}$ ), where indicated. In experiments to test the effect of temperature on synaptic properties, the different temperatures were applied in random order. The slices were viewed using a Nikon (Tokyo, Japan) FN-1 microscope with DIC optics and a Nikon NIR Apo  $\times 40/0.80$  N/A water-immersion objective. The images were collected with a QICLICK, MONO 12BIT camera (Nikon) using NIS-Elements software (Nikon). MOC neurons were identified for whole-cell voltage-clamp recordings by their position in the VNTB (MOC neurons in the dorsal peri-olivary region were not recorded from in this study) and visibility using red epifluorescence (546 nm emission filter, Lumencor Sola lamp). The recordings were performed using a MultiClamp 700B and DigiData 1440A controlled by Clampex 10.6 software (Molecular Devices). The recordings were sampled at 50 kHz and filtered on-line at 10 kHz. The internal solution for MOC recordings contained (in mM): 56 CsCl, 44 CsOH, 49 D-gluconic acid, 1 MgCl<sub>2</sub>, 0.1 CaCl<sub>2</sub>, 10 Hepes, 1 EGTA, 0.3-Na-GTP, 2 Mg-ATP, 3 Na<sub>2</sub>-phosphocreatine, 5 QX-314, 0.25% biocytin, 0.01 AlexaFluor-488 hydrazide. The Cl<sup>-</sup> equilibrium potential was ~−20 mV.

Recording pipettes were pulled from 1.5 mm outer diameter borosilicate glass (Sutter Instrument Co., Novato, CA, USA) to tip resistances of 3–6 M $\Omega$ . Series resistances were corrected 50–85%. The cells were voltage-clamped at −60 mV unless stated otherwise. Membrane voltages were not adjusted for a measured liquid junction potential of −2 mV (caesium gluconate solution). MNTB axons were electrically stimulated to evoke neurotransmitter release and generate postsynaptic currents (PSC) in MOC neurons by a large diameter glass pipette of ~10 or ~30  $\mu\text{m}$  diameter filled with aCSF and 0.01 AlexaFluor-488 hydrazide connected to an Iso-Flex Stimulus Isolation Unit (A.M.P.I., Jerusalem, Israel), placed in the MNTB axon bundle within or at the lateral edge of the MNTB. The stimulus intensity was initially set to zero, then was gradually increased until PSCs were evoked. The stimulus was then adjusted until PSCs were evoked during less than 50% of stimulations, defined as

‘minimal stimulation’. The stimulus intensity was then increased until a maximal evoked PSC (ePSC) amplitude was reached, and then reduced to an intermediate intensity that reliably evoked PSCs at a smaller amplitude than for maximum stimulation,  $320 \pm 180 \mu\text{A}$ . In previous work using the same methodology, this intermediate stimulus intensity evoked PSCs that were approximately 70% of the maximal ePSC amplitude (Torres Cadenas et al., 2020). 6-Cyano-7-nitro-quinoxaline-2,3-dione (CNQX) ( $5 \mu\text{M}$ ) was included in all experiments to block excitatory transmission through AMPA-type glutamate receptors by addition to the recirculating aCSF solution. Drugs and chemicals were obtained from Thermo Fisher Scientific (Waltham, MA, USA) or Sigma-Aldrich (St Louis, MO, USA).

### Experimental design and statistical analysis

Evoked PSC amplitudes were measured in Clampfit 10.6 (Molecular Devices, San Jose, CA, USA) by manually placing cursors at the immediate onset of the PSC (for trains of stimuli, during the decay of the preceding PSC immediately prior to the stimulus artifact), and at the peak of the PSC. The latency to the PSC response was measured from the beginning of the stimulus artifact to the onset of the response. The PSC time constant of decay was measured from the peak of the evoked PSC to the baseline plateau and was fit with a single exponential. In some experiments to measure the effect of spontaneous background activity on synaptic plasticity of inhibitory synaptic inputs, MNTB axons were first stimulated for 20 pulses at 10 or 100 Hz, followed by stimulation at higher rates of 50–500 Hz. The amplitude of ePSCs, probability of recording an evoked PSC, and facilitation index ( $(S_x - S_1)/S_1$ ) was computed during synaptic responses to stimulus trains as in our previous work (Torres Cadenas et al., 2020).

All statistical analyses were performed using Origin v2020 (OriginLab Corp., Northampton, MA, USA) or R version 4.0.2 (R Foundation for Statistical Computing, Vienna, Austria) using packages ‘lme4’ and ‘lmerTest’. Linear mixed models were fit by REML (restricted (residual) maximum likelihood). *t*-Tests used Satterthwaite’s method (‘lmerModLmerTest’). Data were examined for normal distribution using the Shapiro–Wilk test. Non-parametric tests were applied given the non-normal distribution of many variables studied. The differences between two independent groups were assessed using a Mann–Whitney *U*-test. Differences between multiple groups were tested with a Wilcoxon rank sum test. Differences from a defined value of 0 or 1 were tested with a One sample Wilcoxon signed-rank test. To evaluate the effects of stimulation rates on short-term plasticity at MNTB–MOC synapses,

linear mixed-effects models were run with facilitation index as the dependent variable, stimulation rates and trains of electrical stimulation as fixed-effect independent variables. The random effects include random intercept for neurons and random slope for stimulation rate. We used the Akaike information criterion (AIC) to assist with selecting the appropriate statistical model. A lower AIC value indicates better quality of fit. The differences were considered significant if  $P < 0.05$  and indicated by asterisks in figures. For figures, single traces were lowpass filtered at 2 kHz and in cases where more than one voltage-clamp trace was averaged, the data were not filtered. Summary box plots indicate the median and quartiles, with 10 and 90 percentiles indicated by error bars. A square within the box plot indicates the mean. Individual data points are overlaid. All data are presented as median  $\pm$  median absolute deviation (MAD) unless otherwise stated. The figures were prepared in Origin v2020 and Adobe Illustrator CC 2021 (Adobe Inc., San Jose, CA, USA).

### Results

Whole-cell patch-clamp recordings were performed from identified MOC neurons in brain slices from ChAT-IRES-Cre  $\times$  tdTomato mice by targeting red fluorescent neurons in the VNTB. Using this approach, PSCs that were evoked (ePSCs) by electrical stimulation of presynaptic MNTB axons (Fig. 1A) occurred in MOC neurons that were consistent with previous recordings (Torres Cadenas et al., 2020). With the high chloride concentration used here (60 mM), both excitatory and inhibitory PSCs were inward at a holding potential of  $-60$  mV. AMPA receptors were blocked in all experiments with CNQX ( $5 \mu\text{M}$ ) to isolate inhibitory PSCs. After establishing this baseline, we tested whether there was a difference in strength of inhibitory synaptic inputs in male *vs.* female mice. We compared the amplitude of PSCs evoked by minimal stimulation (interpreted as the stimulation of a single axon) and found no difference (ePSC amplitude: female:  $24.4 \pm 7.25$  pA, male:  $28.1 \pm 8.2$ , Mann–Whitney *U*-test,  $U = 302$ ,  $Z = -0.76$ ,  $P = 0.44$ ; ePSC time constant of decay: female:  $11.6 \pm 5.1$  ms, male:  $12.1 \pm 4.5$  ms, Mann–Whitney *U*-test,  $U = 348$ ,  $Z = 0.04487$ ,  $P = 0.96$ ;  $n = 23$  female,  $n = 30$  male). Due to a lack of difference in evoked PSCs of male *vs.* female mice, mice of both sexes were pooled for further analyses.

### Influence of temperature on synaptic plasticity

Previous MOC efferent neuron recordings from our group to characterize MNTB–MOC synapses were performed at room temperature (RT;  $\sim 24^\circ\text{C}$ ) (Torres Cadenas et al., 2020). Because temperature can have diverse effects on

properties of presynaptic vesicle release, postsynaptic responses, and synaptic plasticity, here we compared the effect of a higher, physiological temperature (PhT;  $\sim 35^{\circ}\text{C}$ ), on postsynaptic responses in MOC neurons. During recordings from identified MOC neurons, MNTB axons were stimulated to release neurotransmitter, and ePSCs were measured in the MOC neuron. The amplitude of single ePSCs did not change between RT and PhT (RT amplitude:  $52.8 \pm 26.4$  pA,  $n = 110$  ePSCs in 11 neurons, PhT:  $91.19 \pm 72.02$  pA,  $n = 210$  ePSCs in 21 neurons, Mann–Whitney  $U$ -test,  $U = 100$ ,  $Z = -0.60$ ,  $P = 0.55$ , Fig. 1A–D). However, after MNTB axon stimulation,

MOC neurons had significantly shorter latencies to ePSC onset (RT ePSC latency:  $2.46 \pm 0.73$  ms,  $n = 11$  neurons, PhT:  $1.23 \pm 0.43$  ms,  $n = 21$  neurons, Mann–Whitney  $U$ -test,  $U = 185$ ,  $Z = 2.74$ ,  $P = 0.0062$ , Fig. 1E) and had significantly faster time constants of decay in PhT compared to RT (RT ePSC tau:  $10.97 \pm 3.27$  ms,  $n = 11$  neurons, PhT:  $5.33 \pm 1.82$  ms,  $n = 21$  neurons, Mann–Whitney  $U$ -test,  $U = 198$ ,  $Z = 3.25$ ,  $P = 0.0011$ , Fig. 1F). We next tested the short-term plasticity of MNTB–MOC ePSCs during trains of stimulation of MNTB axons at inter-stimulus intervals (ISIs) from 10 to 100 Hz at RT vs. PhT (Fig. 1G and H). We used the

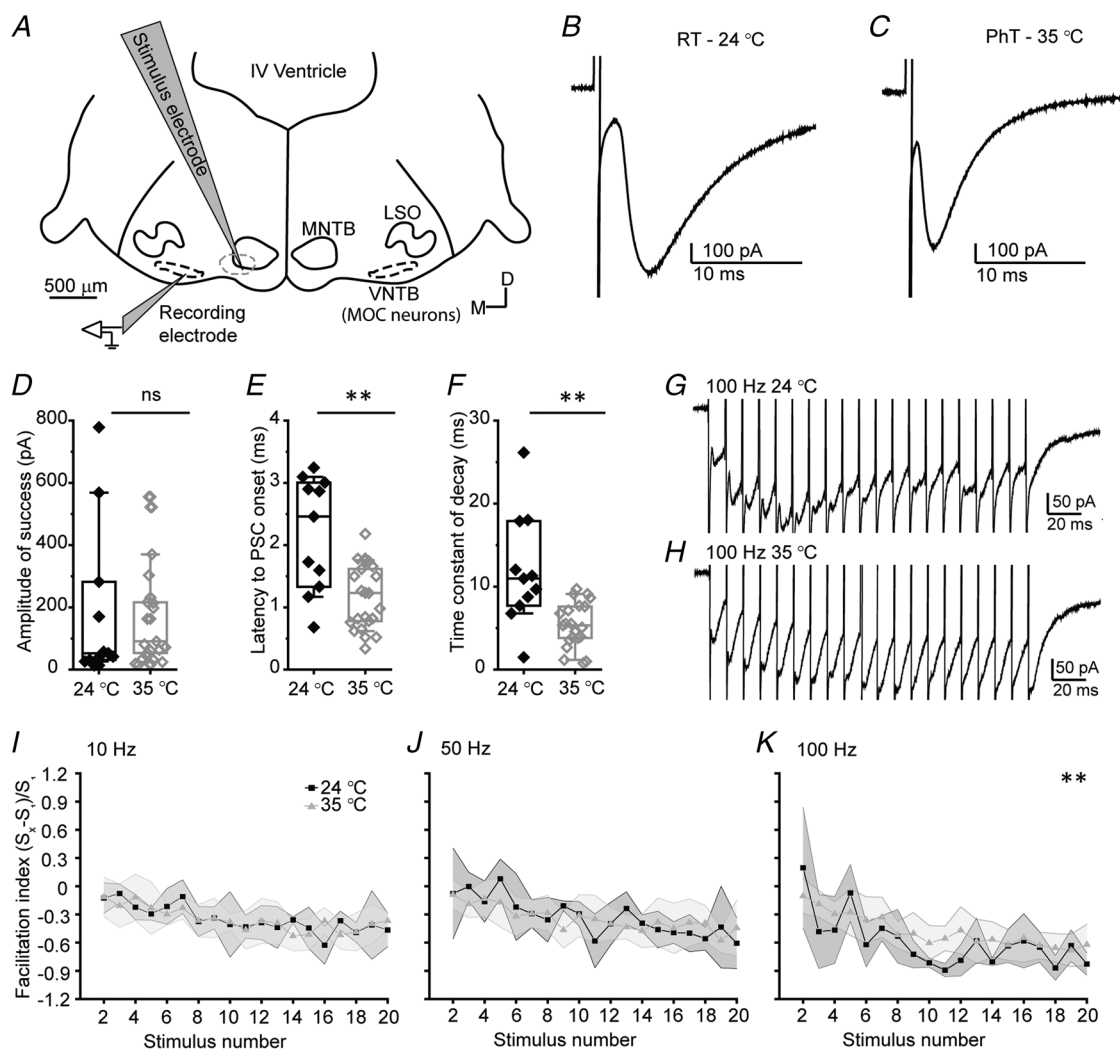


**Figure 1. Temperature dependence of MNTB–MOC synaptic responses**

A, schematic representation of experiments to characterize MNTB–MOC circuitry. B and C, PSCs recorded in identified MOC neurons evoked by electrical stimulation of MNTB axons at RT ( $24^{\circ}\text{C}$ ; B) and PhT ( $35^{\circ}\text{C}$ ; C). D, plot of PSC amplitude at RT and PhT; each data point represents the average from a single cell. E, plot of latency from electrical stimulation of MNTB axons to evoked PSC onset in MOC neurons at RT and PhT. F, plot of time constant of decay of PSCs evoked by electrical stimulation of MNTB axons at RT and PhT. G, example traces of PSCs evoked by 100 Hz stimulation of MNTB axons at RT. H, example traces of PSCs evoked by 100 Hz stimulation of MNTB axons at PhT. I–K, facilitation index by stimulation number of PSCs evoked by stimulation of MNTB axons in RT vs. PhT at 10 Hz (I), 50 Hz (J), and 100 Hz (K). Black, RT; grey, PhT; shading, MAD.

facilitation index to assess short-term synaptic plasticity. Using this index, a positive value indicates synaptic facilitation, and a negative value indicates synaptic depression. We found that the facilitation index was not different across trains of 20 pulses between RT and PhT during 10 or 50 Hz stimulation (10 Hz RT:  $-0.44 \pm 0.11$ ,  $n = 6$  neurons, 10 Hz PhT:  $-0.32 \pm 0.09$ ,  $n = 13$  neurons, Mann–Whitney  $U$ -test:  $U = 136$ ,  $Z = -1.28$ ,  $P = 0.20$ ; 50 Hz RT:  $-0.36 \pm 0.08$ ,  $n = 6$  neurons, 50 Hz PhT:  $-0.34 \pm 0.08$ ,  $n = 13$  neurons, Mann–Whitney  $U$ -test:  $U = 137$ ,  $Z = -1.26$ ,  $P = 0.21$ , Fig. 1I and J). However, at 100 Hz, ePSCs depressed more at RT compared to PhT (100 Hz RT:  $-0.61 \pm 0.13$ ,  $n = 6$  neurons, 100 Hz PhT:  $-0.44 \pm 0.07$ ,  $n = 13$  neurons, Mann–Whitney  $U$ -test:  $U = 56$ ,  $Z = -3.62$ ,  $P = 2.9 \times 10^{-4}$ , Fig. 1K). These results indicate that synaptic activity at MNTB–MOC synapses is more resistant to short-term depression at physiological temperatures.

### Calcium dependence of plasticity at MNTB–MOC synapses

Many auditory neurons in the CN and SOC fire rapid action potentials through the duration of a sound stimulus, so short-term synaptic plasticity due to high rates of synaptic activity has important implications for auditory neuron circuit function. Short-term synaptic plasticity is governed by mechanisms that affect both

pre- and postsynaptic elements, including extracellular calcium concentrations (Neher & Sakaba, 2008; Regehr, 2012). To characterize calcium dependence of short-term synaptic plasticity at the MNTB–MOC synapses, we applied trains of electrical stimulation to MNTB axons at rates of 10–100 ms in extracellular calcium concentrations from 0.5 to 2.0 mM calcium. The effect of stimulation rates was analysed with a linear mixed-effect model. By including random intercept for neurons and random slope for stimulations rate, we assume that the facilitation index and the effect of stimulation rates vary for each neuron. This was the best fitting model (AIC =  $-456.95$ ) compared to a model without random effects (AIC =  $-87.43$ ) and a model with only a random intercept (AIC =  $-279.62$ ). Similar to our previous work (Torres Cadenas et al., 2020), electrical stimulation-evoked PSCs exhibited synaptic depression in 2.0 mM extracellular calcium at stimulation rates of 10, 50 and 100 Hz, with 100 Hz stimulation evoking a significantly greater degree of depression relative to 10 Hz stimulation ( $\beta = -0.35$ , SE: 0.086,  $t = -4.05$ ,  $P = 0.0098$ , Fig. 2Aa). Recent work suggests that an extracellular calcium concentration of 1.2–1.5 mM is thought to approximate *in vivo* levels (Borst, 2010). In 1.2 mM extracellular calcium, trains of stimulation of MNTB axons did not evoke synaptic depression at the second pulse in the train, consistent with previous work using paired pulse stimulation and an ISI of 10 ms (Torres

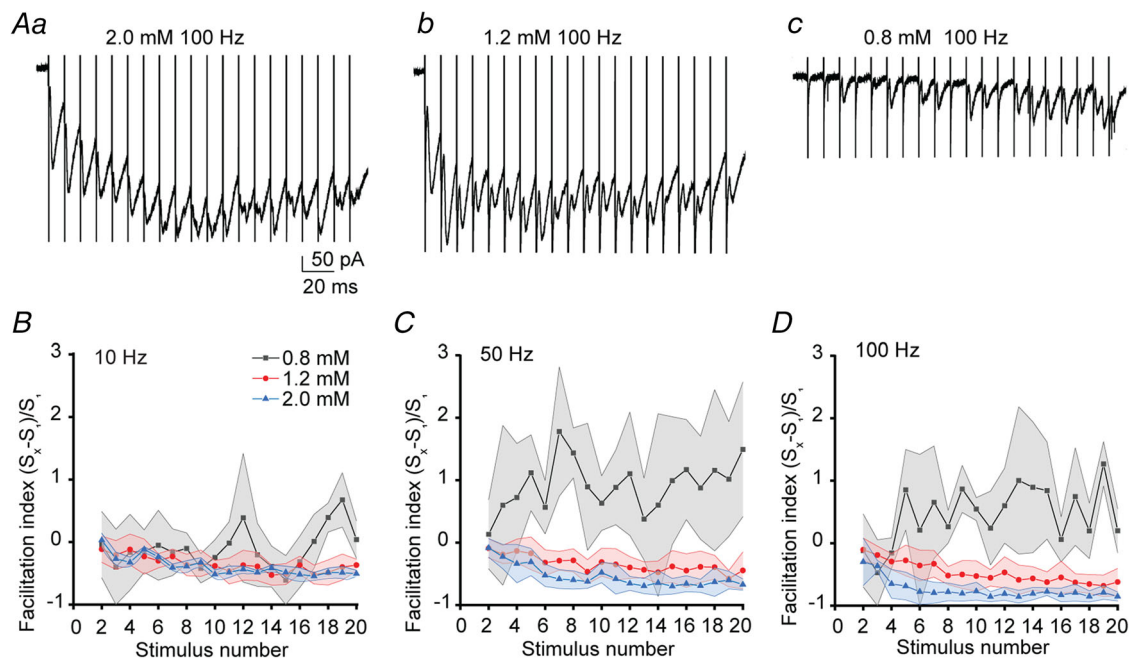


**Figure 2. Calcium dependence of short-term plasticity at MNTB–MOC synapses**

A, ePSCs evoked by trains of electrical stimulation of MNTB axons recorded in high (2.0 mM, a), physiological (1.2 mM, b) and low (0.8 mM, c) extracellular calcium. B–D, facilitation index of PSCs evoked from MNTB axons in 0.8 mM (black), 1.2 mM (red) or 2.0 mM (blue) extracellular calcium, at 10 Hz (B), 50 Hz (C), and 100 Hz (D) stimulation rates. Shading indicates MAD. [Colour figure can be viewed at [wileyonlinelibrary.com](http://wileyonlinelibrary.com)]

Cadenas et al., 2020). However, with sustained synaptic activity through the train, synaptic depression was observed at stimulation rates of 10–100 Hz (one sample Wilcoxon signed-rank test indicated facilitation index was significantly less than zero, index =  $-0.398$ ,  $V = 43,775$ ,  $P < 2.2 \times 10^{-16}$ , Fig. 2*Ab*). Synaptic depression was significantly greater in 2.0 mM compared to 1.2 mM extracellular calcium at train rates of 100 and 50, but not 10 Hz, as measured by facilitation index (100 Hz: 2.0 mM  $-0.299 \pm 0.38$ , 1.2 mM  $-0.105 \pm 0.18$ , Wilcoxon rank sum test  $W = 29,680$ ,  $P = 2.2 \times 10^{-16}$ ; 50 Hz: 2.0 mM  $-0.084 \pm 0.15$ , 1.2 mM  $-0.090 \pm 0.15$ , Wilcoxon rank sum test  $W = 18,780$ ,  $P = 3.4 \times 10^{-7}$ ; 10 Hz: 2.0 mM  $-0.029 \pm 0.11$ , 1.2 mM  $-0.114 \pm 0.21$ , Wilcoxon rank sum test  $W = 19,690$ ,  $P = 0.27$ ,  $n = 6$  neurons, Fig. 2*B–D*). These results indicate that short-term synaptic depression of MNTB–MOC synapses is not as strong in physiological conditions (1.2 mM calcium) compared to higher calcium (2.0 mM) conditions, but synaptic depression in 1.2 mM calcium is significant with sustained synaptic activity.

We further tested the calcium dependence of short-term synaptic plasticity at MNTB–MOC synapses by lowering extracellular calcium concentrations to 0.5 or 0.8 mM. Evoked PSCs were rarely recorded in 0.5 mM calcium (one ePSC in five trains of stimulations each in six neurons, not shown), so synaptic plasticity was not further addressed. However, the rate of PSCs evoked in 0.8 mM extracellular calcium was sufficient to assess plasticity. ePSCs occurred at the first pulse in a train with a lower probability in low (0.8 mM) extracellular calcium compared to 1.2 or 2.0 mM calcium (0.8 mM probability =  $0.2 \pm 0.2$ ,  $n = 8$  neurons, 1.2 mM probability =  $1 \pm 0$ ,  $n = 17$  neurons, 2.0 mM probability =  $1 \pm 0$ ,  $n = 6$  neurons; 0.8 mM vs. 1.2 mM: Mann–Whitney  $U$ -test:  $U = 0$ ,  $Z = -4.34$ ,  $P = 1.43 \times 10^{-5}$ ; 0.8 mM vs. 2.0 mM: Mann–Whitney  $U$ -test:  $U = 0$ ,  $Z = -3.12$ ,  $P = 0.0018$ ). When trains of electrical stimulation were applied to MNTB axons (Fig. 2*Ac*), MNTB–MOC synapses facilitated at stimulation rates of 100 and 50 Hz, but not at 10 Hz (one sample Wilcoxon signed-rank test indicated the facilitation index was significantly greater than zero for 100 and 50 Hz: 100 Hz:  $0.54 \pm 0.33$ ,  $V = 3499.5$ ,  $P = 2.42 \times 10^{-7}$ ; 50 Hz:  $0.89 \pm 0.26$ ,  $V = 5890$ ,  $P = 1.03 \times 10^{-14}$ ; 10 Hz:  $-0.15 \pm 0.16$ ,  $V = 2455.5$ ,  $P = 0.52$ ,  $n = 8$  neurons, Fig. 2*B–D*). These data indicate that extracellular calcium influences short-term synaptic plasticity at the MNTB–MOC synapse.

### Calcium dependence of recovery from short-term plasticity

Following a period of sustained activity that elicits short-term synaptic plasticity, synaptic responses typically

recover to baseline levels with the recovery time indicating when synaptic responses will return to their maximal effect. We investigated recovery of MNTB–MOC synapses after synaptic depression following trains of electrical stimulation of MNTB axons of 20 pulses at 100 Hz, as above, and also probed the calcium dependence of recovery in extracellular calcium concentrations of 1.2 and 2.0 mM. The amplitudes of PSCs evoked by MNTB stimulation were normalized to the first PSC in the train. The facilitation index of the final PSC in the train showed significant depression, as above, but was not different between 1.2 and 2.0 mM calcium (1.2 mM calcium: index =  $-0.56 \pm 0.32$ , Wilcoxon rank sum test  $W = 34$ ,  $Z = 2.17$ ,  $P = 0.030$ ,  $n = 8$  neurons; 2.0 mM: index =  $-0.68 \pm 0.29$ , Wilcoxon rank sum test  $W = 50$ ,  $Z = 2.24$ ,  $P = 0.025$ ,  $n = 10$  neurons, 1.2 vs. 2.0 mM calcium: Mann–Whitney  $U$ -test,  $U = 39.5$ ,  $Z = 0$ ,  $P = 1.00$ ; Fig. 3*A* and *B*). This lack of difference in the facilitation index at the last pulse in the train

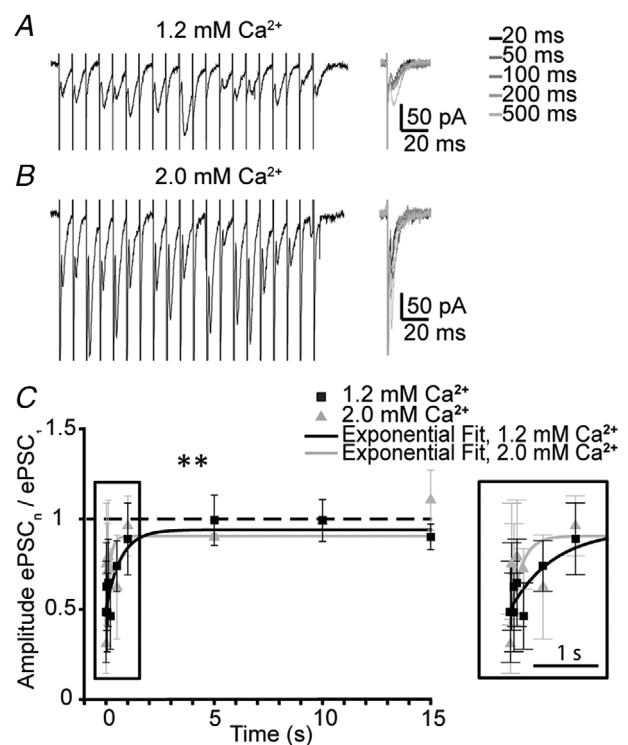


**Figure 3. Calcium dependence of recovery of MNTB–MOC synapses from depression**

*A* and *B*, example PSCs evoked by 100 Hz stimulation in 1.2 mM calcium, followed by PSC evoked after intervals from 20 ms to 500 ms in 1.2 mM (*A*) or 2.0 mM (*B*) extracellular calcium. *C*, amplitude of the average PSC evoked after 20 ms to 15 s recovery following 100 Hz trains of stimulation of MNTB axons, normalized to the first ePSC in the train, in 1.2 (black) or 2.0 (grey) mM extracellular calcium. Curves are exponential fits of the data. Inset shows a zoom of 20 ms to 1 s recovery time points from region indicated by rectangle.



**Table 1. Peak current amplitudes at MNTB–MOC synapses in control conditions and following background MNTB stimulation**

Background stim rate (Hz)	Fast stim rate (Hz)	Peak amplitude control (pA)	Peak amplitude after background stim (pA)	<i>P</i>	<i>n</i> control/background stim
10	50	276.9 ± 102.7	227.2 ± 172.25	0.78	15/8
10	100	407.05 ± 182.55	363.4 ± 218.6	0.52	20/7
10	200	390 ± 119.7	264.5 ± 83.1	0.69	13/7
100	200	160.74 ± 119.7	81.91 ± 17.9	0.0033	13/6
100	500	500.35 ± 99.05	80.15 ± 18.9	0.0508	8/4

Data are presented as median ± MAD. Fast rates of MNTB axon stimulation were applied at the rates indicated ('sound-like' stimulation rate), either in control conditions or following two seconds of mild (10 Hz) or strong (100 Hz) background stimulation.

indicates that the synapses recovered from a similar degree of synaptic depression in both 1.2 and 2.0 mM calcium. Following the last pulse in the train, MNTB axons were again stimulated after a recovery interval ranging from 20 ms to 15 s (Fig. 3A and B). The amplitudes of PSCs evoked after the recovery interval were normalized to the first PSC in the original 100 Hz train. Evoked PSCs recovered to baseline values after about 1 s, with a faster time constant of recovery in 2.0 mM compared to 1.2 mM calcium (recovery time constant: 1.2 mM Ca<sup>2+</sup>: 470.10 ± 208.47 ms, *n* = 7–9 cells per interval; 2.0 mM Ca<sup>2+</sup>: 118.13 ± 65.36 ms, *n* = 5–7 cells per interval; ePSC ~  $\alpha \exp(\text{time} \times \beta) + \theta$ , larger magnitude of  $\beta$  indicates steeper decay: 1.2 mM Ca<sup>2+</sup>  $\beta$  = -2.1 ± 1.6 SE, 2.0 mM Ca<sup>2+</sup>  $\beta$  = -35.5 ± 28.1 SE, *P* = 0.0244, Fig. 3C and inset), demonstrating a calcium dependence of recovery from synaptic depression.

### MNTB–MOC synaptic function following tonic background MNTB activity

MNTB neurons have a high background firing rate up to 189 Hz in the absence of sound, with average rates around 10–20 Hz documented in multiple species (Hermann et al., 2007; Kadner & Berrebi, 2008; Kopp-Scheinflug et al., 2003, 2008; Smith et al., 1998; Sommer et al., 1993). This high rate of background firing suggests that the MNTB–MOC synapses may be tonically depressed *in vivo*, even in quiet. Therefore, we mimicked the tonic activity level present *in vivo* at the MNTB–MOC synapse to determine if this baseline activity could alter ePSCs in MOC neurons at faster activity rates, such as might occur during the transition from quiet to sound-driven activity. Experiments were performed in 1.2 mM extracellular calcium and at physiological temperature. To mimic tonic firing, we applied 'background' stimulation to MNTB axons at 10 Hz, a typical spontaneous rate for MNTB neurons. This firing rate evokes mild synaptic depression at MNTB–MOC synapses, while a high rate of baseline

stimulation at 100 Hz evokes strong synaptic depression at the MNTB–MOC synapse, as shown above. After 2 s of mild (10 Hz) or strong (100 Hz) baseline stimulation we then applied a 400 ms stimulation, at 50, 100, 200 or 500 Hz, to mimic enhanced MNTB synaptic activity associated with sound (Fig. 4A and B). We compared the peak current amplitude reached in the control condition to the peak current amplitude reached following background stimulation. Mild background stimulation at 10 Hz did not reduce the subsequent responses to faster stimulation, but faster (100 Hz) background stimulation inhibited the response to subsequent stimulation at 200 Hz (Fig. 4C–G and Table 1). Thus, if a given MNTB neuron has a typical, mild rate of background activity, the MNTB synapse will have a significant effect on the MOC neuron at sound onset. However, for the MNTB neurons with a high background activity, further synaptic activity evoked by sound may have a limited effect on the postsynaptic MOC neuron.

### Rapid, sustained activity at MNTB–MOC synapses

Sound-driven responses of MNTB neurons *in vivo* can be up to 500–700 Hz (Kopp-Scheinflug et al., 2008). Because MNTB–MOC synapses depress during repetitive stimulation, we asked whether these synapses can maintain activity even when rapid stimulation rates are applied for sustained durations. For this work we applied trains of electrical stimulation to MNTB axons at rates of 200 and 500 Hz for a duration of 1 s. During this sustained stimulation we found that evoked responses summated and became indistinct over the duration of the trains to reach a peak amplitude that incorporated both summation and short-term plasticity (Fig. 5A and B). The peak amplitude was not different between 200 and 500 Hz stimulation rates (peak amplitude: 200 Hz: 395.90 ± 158.5 pA, *n* = 5 neurons; 500 Hz: 519.25 ± 225.3 pA, *n* = 6 neurons, Mann–Whitney *U*-test: *U* = 13, *Z* = -0.27, *P* = 0.78, Fig. 5C). Although there was no change in

peak amplitude, there was a trend towards a faster latency from stimulation onset to peak in MNTB–MOC synapses stimulated at 500 compared to 200 Hz (latency to peak: 200 Hz:  $45.36 \pm 11.09$  ms,  $n = 5$  neurons; 500 Hz:  $26.44 \pm 8.46$  ms,  $n = 6$  neurons, Mann–Whitney  $U$ -test:  $U = 26$ ,  $Z = 1.92$ ,  $P = 0.055$ , Fig. 5D). Following this peak in activity, the total current had an exponential decay with a time constant that was not different between stimulation rates (200 Hz exponential decay:  $715.92 \pm 106.31$  ms,  $n = 5$  neurons, 500 Hz decay:  $447.23 \pm 277.47$  ms,  $n = 6$  neurons, Mann–Whitney  $U$ -test:  $U = 15$ ,  $Z = 0.42$ ,  $P = 0.68$ , Fig. 5E) and also decayed to a plateau current that was not different between stimulation rates (plateau current: 200 Hz:  $92.4 \pm 35.2$  pA,  $n = 5$  neurons, 500 Hz plateau:  $144.6 \pm 93.8$  pA,  $n = 6$  neurons, Mann–Whitney  $U$ -test:  $U = 10$ ,  $Z = -0.82$ ,  $P = 0.41$ ). Thus, during sustained MNTB–MOC synapse activity such as may occur during a sustained sound, the evoked responses build to a peak followed by decay but are able to maintain a sustained inhibitory current.

## Discussion

Functional evidence describing the complexity of synaptic inputs to MOC neurons corroborates existing histological evidence that multiple classes of neurons form synapses onto olivocochlear efferent neurons, indirectly influencing cochlear function. Recent work demonstrates that MOC neurons are excited by both ascending sound-driven inputs from CN T-stellate and small cell cap cells and descending excitation from the IC (Hockley et al., 2022; Romero & Trussell, 2021). MOC neurons are also inhibited by ascending sound-driven pathways via MNTB neurons (Torres Cadenas et al., 2020). There are likely additional sources of excitation, inhibition, or modulation from auditory and other brain regions as indicated by histological studies (Brown et al., 2013; Caicedo & Herbert, 1993; Faye-Lund, 1986; Gómez-Nieto, Rubio et al., 2008; Groff & Liberman, 2003; Horvath et al., 2003; Mulders & Robertson, 2000, 2002; Ota et al., 2004; Suthakar & Ryugo, 2017; Thompson & Thompson, 1993; Vetter et al., 1993). The integration of these synaptic inputs

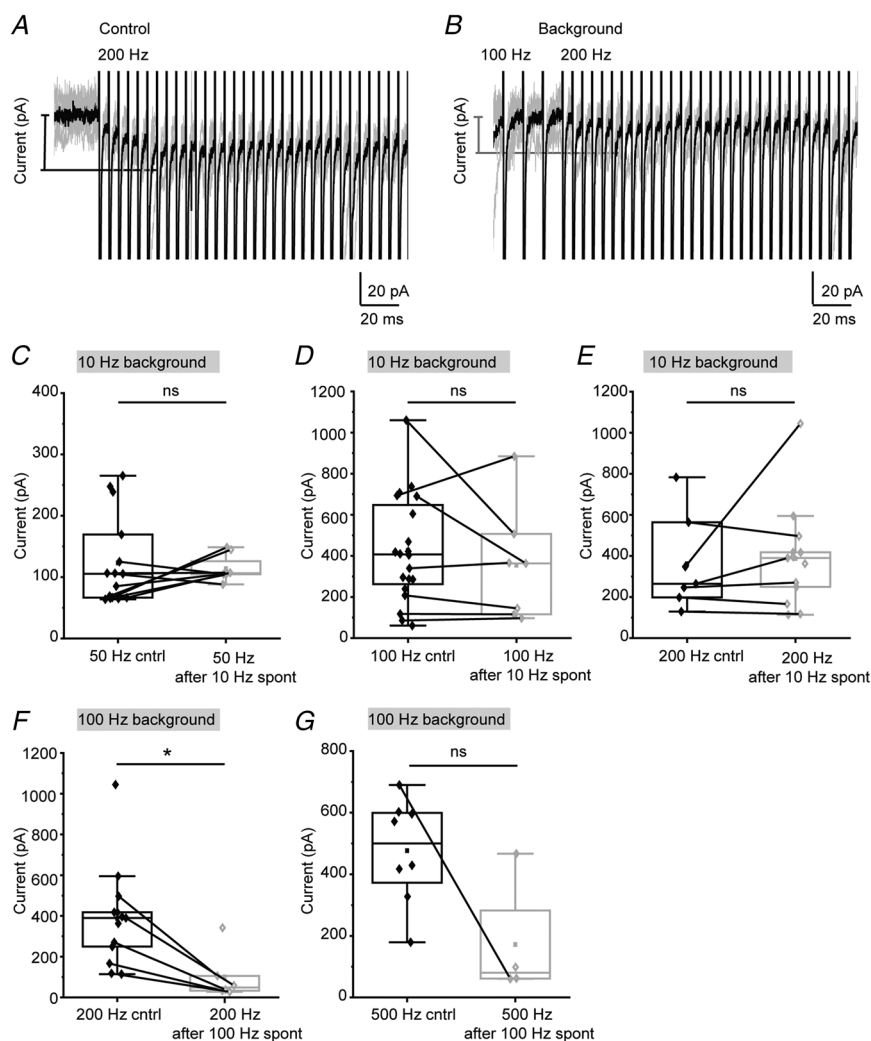


**Figure 4. High rates of background MNTB synaptic activity reduce responses to subsequent activity**

**A**, example voltage clamp trace showing the response of an MOC neuron to 200 Hz stimulation of MNTB axons. Grey, individual traces; black, average trace. Vertical lines are the stimulation artifact. **B**, same neuron as in **A**, response to 100 Hz background stimulation of MNTB axons followed by 200 Hz stimulation. **C–E**, plots showing the peak current measured as in **A** and **B** during trains of MNTB axon stimulation either in control conditions or following 10 Hz background stimulation of MNTB axons. Lines connect datapoints from the same neuron. **F–G**, plots showing the peak current measured as in **A** and **B** during trains of MNTB axon stimulation either in control conditions or following 100 Hz background stimulation of MNTB axons. Lines connect datapoints from the same neuron.

to govern MOC activity depend on the relative strength and postsynaptic effect of inputs, and their plasticity during changing hearing conditions. Here we further characterize the short-term plasticity of inhibitory inputs to MOC neurons from neurons of the MNTB, in mouse. MNTB–MOC synaptic inputs depress over a range of physiological calcium and stimulation rate conditions, yet maintain sustained synaptic function. This holds even during high rates of activity and following background spontaneous rates of activity.

### Temperature and calcium effects on MNTB–MOC plasticity

Increasing the temperature of tissue speeds the kinetics of biological processes, including those regulating vesicular neurotransmitter release (Sabatini & Regehr, 1996).

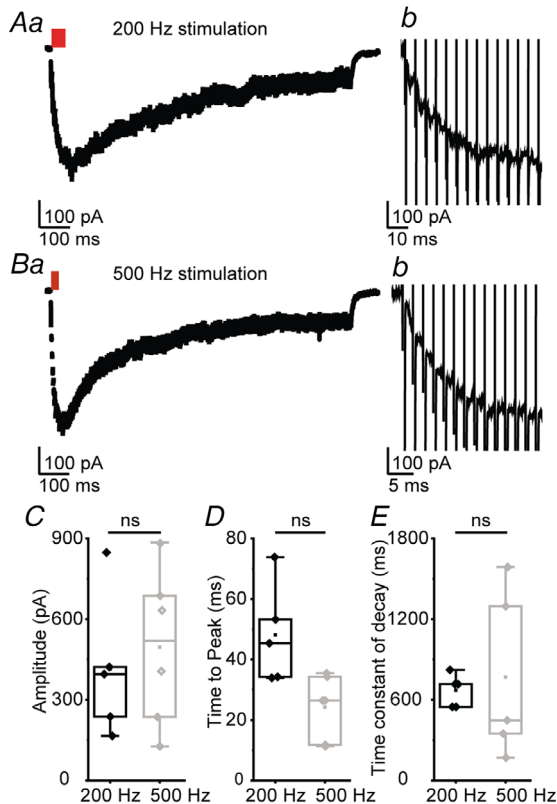


**Figure 5. High frequency activation of MNTB–MOC axons evokes strong synaptic depression followed by tonic activity**  
*Aa*, example trace showing MOC neuron response to 200 Hz stimulation of MNTB axons. Stimulus artifacts were digitally removed. *Ab*, zoom of trace shown by red in *Aa*. *Ba*, example trace showing response to 500 Hz stimulation of MNTB axons. Stimulus artifacts were digitally removed. *Bb*, zoom of trace shown by red in *Ba*. *C*, plot of peak amplitude of summated ePSCs evoked by stimulation of MNTB axons at 200 or 500 Hz. *D*, plot of time to peak of summated ePSCs evoked by stimulation of MNTB axons at 200 or 500 Hz. *E*, time constant of decay of summated ePSCs evoked by stimulation of MNTB axons at 200 or 500 Hz. [Colour figure can be viewed at [wileyonlinelibrary.com](http://wileyonlinelibrary.com)]

Consistent with this idea, raising the temperature of a brain slice from RT to PhT during patch-clamp recordings of MNTB–MOC synaptic responses both decreased the latency and sped up the kinetics of evoked PSCs. Using PhT during recording has also been shown to decrease the latency and speed of evoked PSCs in neurons from other auditory and non-auditory brain areas (Kushmerick et al., 2006; Taschenberger & von Gersdorff, 2000; Zhang & Trussell, 1994). However, we saw no change in the amplitude of single evoked PSCs in PhT compared to RT. In other cell types an increase in evoked PSC amplitudes with increased temperature has been observed (Hardingham & Larkman, 1998; Kushmerick et al., 2006; Taschenberger & von Gersdorff, 2000; Zhang & Trussell, 1994), sometimes also associated with an increase in the mini-PSC (mPSC) amplitude (Kushmerick et al., 2006; Van Hook, 2020). In other systems that also have an increase in evoked PSC amplitude with increased temperature, this effect was not associated with an increase in mPSC amplitude (Hardingham & Larkman, 1998). It is unclear why we do not see an increased PSC amplitude with temperature. This may simply reflect a lack of change in quantal size with temperature combined with fewer release sites from MNTB onto MOC neurons, especially compared to other studies discussed here that examined synapses with many release sites.

Changes in short-term synaptic plasticity with temperature have been observed at other central synapses. While many mechanisms affect both pre- and postsynaptic plasticity, net plasticity can be in part attributed to a balance between release probability and vesicle recruitment. Release probability has been observed to increase with temperature at many (Hardingham & Larkman, 1998; Pyott & Rosenmund, 2002; Volgushev et al., 2004) but not all (Allen & Stevens, 1994) synapses and is typically associated with increased synaptic depression. Increased vesicle recruitment occurs with increased temperature (Kushmerick et al., 2006; Pyott & Rosenmund, 2002) and is associated with decreased synaptic depression. However, at many synapses the net effect is a reduction in short-term synaptic depression at PhT relative to RT (Brenowitz et al., 1998; Hardingham & Larkman, 1998; Kushmerick et al., 2006; Pyott & Rosenmund, 2002; Taschenberger & von Gersdorff, 2000; Volgushev et al., 2004). Consistent with these studies, we find that there is less synaptic depression of MNTB–MOC synapses at PhT compared to RT, extending this principle to inhibitory synapses.

In addition to temperature effects, short-term synaptic plasticity involves interplay between many mechanisms, including presynaptic calcium dynamics, vesicle and release site properties, neurotransmitter diffusion and clearance from the synaptic cleft, and postsynaptic receptor dynamics, among other mechanisms. Various mechanisms for the strong influence of extracellular

calcium on presynaptic mechanisms of plasticity have been proposed, including vesicle pool replenishment or depletion, changes in vesicle release probability, and effects on presynaptic calcium channels (Catterall & Few, 2008; Fioravante & Regehr, 2011; Mochida, 2011; Neher & Sakaba, 2008; Sakaba et al., 2002; Zucker & Regehr, 2002; reviewed in Regehr, 2012). In our previous work there was no difference between short term depression at MNTB–MOC synapses in 2.0 vs. 1.2 mM calcium when measured with paired pulse stimulation (Torres Cadenas et al., 2020), suggesting that synaptic plasticity is independent of extracellular calcium at this synapse. While unusual, this has been observed at other auditory synapses in the CN that were tested with high vs. physiological (lower) divalent cations in aCSF (Xie & Manis, 2017). However, extending the duration of synaptic activity to trains of stimulation of MNTB–MOC synapses demonstrated less synaptic depression in 1.2 compared to 2.0 mM calcium. With a further decrease in the calcium concentration to 0.8 mM, MNTB–MOC synapses were facilitated, confirming the calcium dependence of plasticity at the MNTB–MOC synapse via an unknown mechanism at the MNTB axon terminal.

The recovery of a synapse from depression is also calcium dependent, including dependence on mechanisms such as vesicle pool refilling (Dittman & Regehr, 1998; Neher & Sakaba, 2008). Indeed, MNTB–MOC synapses recovered to baseline levels faster in higher calcium conditions. Interestingly, the time constant of recovery from depression of inhibitory synapses to MOC neurons was faster than that of excitatory synapses to MOC neurons from either T-stellate or inferior colliculus neurons (Romero & Trussell, 2021). This suggests that if excitatory and inhibitory inputs to MOC neurons experience similar activity rates, inhibitory synapses will recover from depression faster than excitatory synapses.

### Effect of spontaneous background activity on MNTB–MOC synaptic inhibition

The GBC–MNTB pathway that inhibits MOC neurons is remarkably fast and powerful, with high-fidelity synaptic transfer in response to stimulation up to ~800 Hz at the calyx of Held synapse *in vitro* (Futai et al., 2001; Joshi et al., 2004; Kopp-Scheinflug et al., 2003; Spirou et al., 1990; Taschenberger & von Gersdorff, 2000; Wu et al., 1993). *In vivo*, the background spontaneous rate of MNTB activity in the absence of sound averages about 10–20 Hz and can range up to 190 Hz (Hermann et al., 2007; Kadner et al., 2006; Kopp-Scheinflug et al., 2003, 2008; Smith et al., 1998; Sommer et al., 1993). In response to sound stimulation, MNTB neurons have a primary-like with notch firing pattern (Guinan & Li, 1990;

Kopp-Scheinflug et al., 2008; Paolini et al., 2001; Smith et al., 1998; Tolnai et al., 2009) and spike at rates of up to hundreds of hertz *in vivo* (Kopp-Scheinflug et al., 2008). Work from other labs has demonstrated that the calyx of Held synapses onto MNTB neurons have smaller evoked responses and more action potential failures following spontaneous background activity, but exhibit less synaptic depression during fast trains (Hermann et al., 2007). In addition, there is a transient synaptic facilitation following background stimulation (Müller et al., 2010). The *in vivo* activity patterns of MNTB–MOC synapses are unknown, but we assumed that, similar to the MNTB soma, they may have some baseline spontaneous activity that evokes tonic depression, followed by faster rates of activity in response to sound. MNTB inhibition of MOC neurons was not reduced by a low, 10 Hz background synaptic stimulation rate, but was reduced by a prior high, 100 Hz synaptic stimulation rate. Therefore, most MNTB neurons with low background spontaneous rates will likely inhibit MOC neurons upon sound onset. In contrast, MNTB neurons with high background activity levels may instead exert a tonic inhibition of MOC neurons that prevents MOC activity except during a strong sound stimulus.

### Effect of inhibition on MOC activity

MOC neurons in guinea pig and cat rarely fire action potentials in quiet *in vivo*, and have low threshold responses to acoustic stimuli (Liberman, 1988; Liberman & Brown, 1986; Robertson, 1984; Robertson & Gummer, 1985). In contrast, in young mice (P14–P23), post-hearing onset MOC neurons sometimes have spontaneous action potentials *in vitro* (Torres Cadenas et al., 2020). MOC neurons recorded from brain slices of mice older (P30–P48) than those used in the present study lack spontaneous action potentials (Romero & Trussell, 2021). Activity from inhibitory MNTB inputs is likely silent in these experiments on more mature mice because spontaneous activity from MNTB neurons is largely absent in *in vitro* brain slices (Hermann et al., 2007). This suggests that changes in intrinsic electrical properties that occur with maturation, not inhibition, are likely responsible for the low spontaneous spike rate of mature MOC neurons *in vivo*, although evoked inhibition from the MNTB persists in the mature MOC neurons at the same levels as in younger animals (Torres Cadenas et al., 2020).

Instead of controlling the MOC neuron resting membrane potential, inhibition from MNTB neurons likely has a primary role in modulating MOC neuron responses to sound-driven excitatory synaptic inputs. We propose a model in which low rates of spontaneous MNTB–MOC synaptic activity in quiet provides mild inhibition and electrical shunting of MOC neurons that

may raise the action potential threshold in response to excitation. Higher rates of MNTB–MOC activity at sound onset suppress and delay MOC responses to concurrent excitatory synaptic inputs, consistent with the long and variable latencies (from ~5 to ~65 ms) of MOC neurons in response to sound (Liberman & Brown, 1986; Robertson, 1984; Robertson & Gummer, 1985). Indeed, 100 Hz, but not slower, stimulation of MNTB axons using the same methodology as in the current work delays spontaneous MOC action potentials (Torres Cadenas et al., 2020). Through a long-duration sound, the MNTB–MOC synapses would undergo short-term depression that reduces the influence of inhibition. The time course of decay of sustained MNTB–MOC inhibition is in the range of hundreds of milliseconds, which is too long to account for the spike latencies of MOC neuron sound responses. Therefore, activation of MOC neurons by both ascending excitatory drive from the CN (Hockley et al., 2022; Romero & Trussell, 2021) and descending, facilitating excitation from the IC (Romero & Trussell, 2021) likely overcomes inhibition to evoke action potentials in MOC neurons. This hypothesized interaction of excitation and inhibition in MOC neurons, combined with the low synaptic release probability and subsequent facilitation of MOC effects on cochlear OHCs (Ballesterro et al., 2011), is consistent with the build-up of ‘fast’ MOC effects as measured by distortion product otoacoustic emissions (~100 ms; Guinan, 2011). However, this model does not inform ‘slow’ MOC effects lasting seconds (Guinan, 2011), which is likely due to properties of excitatory and modulatory synaptic inputs to MOC neurons. In contrast to the majority of MOC neurons that are likely receiving low rates of spontaneous background MNTB synaptic activity, MOC neurons receiving high rates of spontaneous background MNTB synaptic activity are likely insensitive to moderate sound. However, MOC neurons with rapid background inhibition may have a short latency response to onset of a loud sound due to the tonic synaptic depression of their inhibitory synaptic inputs. This is consistent with *in vivo* work showing a decrease in MOC response latency with increased sound intensity (Liberman & Brown, 1986). Therefore, reduced inhibitory drive to a subpopulation of MOC neurons at sound onset due to high rates of tonic inhibitory synaptic activity and subsequent depression may allow for faster negative feedback to the cochlea in response to loud sounds. Overall, inhibitory synapses from the MNTB to the MOC are likely characterized by tonic activity that under most conditions of low background activity would continuously inhibit MOC function in quiet, and robustly inhibit MOC neuron function at sound onset. These functions combine to delay MOC suppression of cochlear activity during rapidly modulating sound.

## References

- Allen, C., & Stevens, C. F. (1994). An evaluation of causes for unreliability of synaptic transmission. *PNAS*, **91**(22), 10380–10383.
- Art, J. J., Crawford, A. C., Fettiplace, R., & Fuchs, P. A. (1985). Efferent modulation of hair cell tuning in the cochlea of the turtle. *Journal of Physiology*, **360**(1), 397–421.
- Ballesterro, J., Zorrilla de San Martín, J., Goutman, J. D., Elgoyhen, A. B., Fuchs, P. A., Katz, E., & Zorrilla de San Martín, J. (2011). Short-term synaptic plasticity regulates the level of olivocochlear inhibition to auditory hair cells. *Journal of Neuroscience*, **31**(41), 14763–14774.
- Banks, M. I., & Smith, P. H. (1992). Intracellular recordings from neurobiotin-labeled cells in brain slices of the rat medial nucleus of the trapezoid body. *Journal of Neuroscience*, **12**(7), 2819–2837.
- Barnes-Davies, M., & Forsythe, I. D. (1995). Pre- and post-synaptic glutamate receptors at a giant excitatory synapse in rat auditory brainstem slices. *Journal of Physiology*, **488**(2), 387–406.
- Boero, L. E., Castagna, V. C., Di Guilmi, M. N., Goutman, J. D., Belén Elgoyhen, A., & Gómez-Casati, M. E. (2018). Enhancement of the medial olivocochlear system prevents hidden hearing loss. *Journal of Neuroscience*, **38**(34), 7440–7451.
- Borst, J. G., Helmchen, F., & Sakmann, B. (1995). Pre- and postsynaptic whole-cell recordings in the medial nucleus of the trapezoid body of the rat. *Journal of Physiology*, **489**(3), 825–840.
- Borst, J. G. G. (2010). The low synaptic release probability in vivo. *Trends in Neuroscience*, **33**(6), 259–266.
- Brenowitz, S., David, J., & Trussell, L. (1998). Enhancement of synaptic efficacy by presynaptic GABA(B) receptors. *Neuron*, **20**(1), 135–141.
- Brown, M. C. (1989). Morphology and response properties of single olivocochlear fibers in the guinea pig. *Hearing Research*, **40**(1–2), 93–109.
- Brown, M. C., de Venecia, R. K., & Guinan, J. J. (2003). Responses of medial olivocochlear neurons. Specifying the central pathways of the medial olivocochlear reflex. *Experimental Brain Research*, **153**(4), 491–498.
- Brown, M. C., Mukerji, S., Drottar, M., Windsor, A. M., & Lee, D. J. (2013). Identification of inputs to olivocochlear neurons using transneuronal labeling with pseudorabies virus (PRV). *Journal of the Association for Research in Otolaryngology*, **14**(5), 703–717.
- Caicedo, A., & Herbert, H. (1993). Topography of descending projections from the inferior colliculus to auditory brainstem nuclei in the rat. *Journal of Comparative Neurology*, **328**(3), 377–392.
- Catterall, W. A., & Few, A. P. (2008). Calcium channel regulation and presynaptic plasticity. *Neuron*, **59**(6), 882–901.
- Chen, E., Lallai, V., Sherfat, Y., Grimes, N. P., Pushkin, A. N., Fowler, J. P., & Fowler, C. D. (2018). Altered baseline and nicotine-mediated behavioral and cholinergic profiles in ChAT-Cre mouse lines. *Journal of Neuroscience*, **38**(9), 2177–2188.

- Christian Brown, M., Lee, D. J., & Benson, T. E. (2013). Ultrastructure of spines and associated terminals on brainstem neurons controlling auditory input. *Brain Research*, **1516**, 1–10.
- Darrow, K., Benson, T. E., & Brown, M. C. (2012). Planar multipolar cells in the cochlear nucleus project to medial olivocochlear neurons in mouse. *Journal of Comparative Neurology*, **520**(7), 1365–1375.
- De Venecia, R. K., Liberman, M. C., Guinan, J. J., & Brown, M. C. (2005). Medial olivocochlear reflex interneurons are located in the posteroventral cochlear nucleus: A kainic acid lesion study in guinea pigs. *Journal of Comparative Neurology*, **487**(4), 345–360.
- Delano, P. H., Elgueta, D., Hamame, C. M., & Robles, L. (2007). Selective attention to visual stimuli reduces cochlear sensitivity in chinchillas. *Journal of Neuroscience*, **27**(15), 4146–4153.
- Desmedt, J. (1962). Auditory-evoked potentials from cochlea to cortex as influenced by activation of the efferent olivo-cochlear bundle. *Journal of the Acoustical Society of America*, **34**(9B), 1478–1496.
- Dittman, J. S., & Regehr, W. G. (1998). Calcium dependence and recovery kinetics of presynaptic depression at the climbing fiber to purkinje cell synapse. *Journal of Neuroscience*, **18**(16), 6147–6162.
- Faye-Lund, H. (1986). Projection from the inferior colliculus to the superior olivary complex in the albino rat. *Anatomy and Embryology*, **175**(1), 35–52.
- Fex, J. (1962a). Auditory activity in centrifugal and centripetal cochlear fibres in cat. A study of a feedback system. *Acta Physiologica Scandinavica Supplementum*, **189**, 1–68.
- Fex, J. (1962b). Single fibre analysis of crossed efferent fibres. *Acta Physiologica Scandinavica*, **55**, 7–32.
- Fioravante, D., & Regehr, W. G. (2011). Short-term forms of presynaptic plasticity. *Current Opinion in Neurobiology*, **21**(2), 269–274.
- Friauf, E., & Ostwald, J. (1988). Divergent projections of physiologically characterized rat ventral cochlear nucleus neurons as shown by intra-axonal injection of horseradish peroxidase. *Experimental Brain Research*, **73**(2), 263–284.
- Fuchs, P. A., & Lauer, A. M. (2019). Efferent inhibition of the cochlea. *Cold Spring Harbor perspectives in medicine*, **9**(5), 1–16.
- Futai, K., Okada, M., Matsuyama, K., & Takahashi, T. (2001). High-fidelity transmission acquired via a developmental decrease in NMDA receptor expression at an auditory synapse. *Journal of Neuroscience*, **21**(10), 3342–3349.
- Galambos, R. (1956). Suppression of auditory nerve activity by stimulation of efferent fibers to cochlea. *Journal of Neurophysiology*, **19**(5), 424–437.
- Geisler, C. D. (1974). Letter: Hypothesis on the function of the crossed olivocochlear bundle. *Journal of the Acoustical Society of America*, **56**(6), 1908–1909.
- Glendenning, K. K., Brusno-Bechtold, J. K., Thompson, G. C., & Masterton, R. B. (1981). Ascending auditory afferents to the nuclei of the lateral lemniscus. *Journal of Comparative Neurology*, **197**(4), 673–703.
- Glenn, J., & Oatman, L. (1977). Effects of visual attention on the latency of auditory evoked potentials. *Experimental Neurology*, **57**(1), 34–40.
- Gómez-Nieto, R., Horta-Junior, J. A. C., Castellano, O., Herrero-Turrión, M. J., Rubio, M. E., & López, D. E. (2008). Neurochemistry of the afferents to the rat cochlear root nucleus: possible synaptic modulation of the acoustic startle. *Neuroscience*, **154**(1), 51–64.
- Gómez-Nieto, R., Rubio, M. E., & López, D. E. (2008). Cholinergic input from the ventral nucleus of the trapezoid body to cochlear root neurons in rats. *Journal of Comparative Neurology*, **506**(3), 452–468.
- Groff, J. A., & Liberman, M. C. (2003). Modulation of cochlear afferent response by the lateral olivocochlear system: activation via electrical stimulation of the inferior colliculus. *Journal of Neurophysiology*, **90**(5), 3178–3200.
- Guinan, J. J. (1996). Physiology of olivocochlear efferents. In P. Dallos, R. Fay, & A. Popper (eds.), *The Cochlea: Springer handbook of auditory research* (pp 435–502). Springer-Verlag.
- Guinan, J. J. (2011). Physiology of the medial and lateral olivocochlear systems. In D. K. Ryugo, R. Fay, & A. Popper, (eds.), *Auditory and vestibular efferents; Springer Handbook of Auditory Research* (pp 39–81). Springer Handbook of Auditory Research.
- Guinan, J. J., & Gifford, M. L. (1988). Effects of electrical stimulation of efferent olivocochlear neurons on cat auditory-nerve fibers. III. Tuning curves and thresholds at CF. *Hearing Research*, **37**(1), 29–45.
- Guinan, J. J., & Li, R. Y. (1990). Signal processing in brainstem auditory neurons which receive giant endings (calyces of Held) in the medial nucleus of the trapezoid body of the cat. *Hearing Research*, **49**(1–3), 321–334.
- Hardingham, N. R., & Larkman, A. U. (1998). The reliability of excitatory synaptic transmission in slices of rat visual cortex in vitro is temperature dependent. *Journal of Physiology*, **507**(1), 249–256.
- Held, H. (1893). Die centrale Gehörleitung. *Archiv für Anatomie, Physiologie*, 201–247.
- Hermann, J., Pecka, M., von Gersdorff, H., Grothe, B., & Klug, A. (2007). Synaptic transmission at the calyx of Held under in vivo like activity levels. *Journal of Neurophysiology*, **98**(2), 807–820.
- Hockley, A., Wu, C., & Shore, S. E. (2022). Olivocochlear projections contribute to superior intensity coding in cochlear nucleus small cells. *Journal of Physiology*, **600**(1), 61–73.
- Horvath, M., Ribári, O., Répássy, G., Tóth, I. E., Boldogkői, Z., Palkovits, M. M., Ribari, O., Repassy, G., Toth, I. E., Boldogkoi, Z., & Palkovits, M. M. (2003). Intracochlear injection of pseudorabies virus labels descending auditory and monoaminergic projections to olivocochlear cells in guinea pig. *European Journal of Neuroscience*, **18**(6), 1439–1447.
- Joshi, I., Shokralla, S., Titis, P., & Wang, L.-Y. (2004). The role of AMPA receptor gating in the development of high-fidelity neurotransmission at the calyx of Held synapse. *Journal of Neuroscience*, **24**(1), 183–196.
- Kadner, A., & Berrebi, A. S. (2008). Encoding of temporal features of auditory stimuli in the medial nucleus of the trapezoid body and superior paraolivary nucleus of the rat. *Neuroscience*, **151**(3), 868–887.

- Kadner, A., Kulesza, R. J., & Berrebi, A. S. (2006). Neurons in the medial nucleus of the trapezoid body and superior paraolivary nucleus of the rat may play a role in sound duration coding. *Journal of Neurophysiology*, **95**(3), 1499–1508.
- Kawase, T., Delgutte, B., & Liberman, M. C. (1993). Anti-masking effects of the olivocochlear reflex. II. Enhancement of auditory-nerve response to masked tones. *Journal of Neurophysiology*, **70**(6), 2533–2549.
- Kopp-Scheinflug, C., Lippe, W. R., Dörrscheidt, G. J., & Rübsamen, R. (2003). The medial nucleus of the trapezoid body in the gerbil is more than a relay: Comparison of pre- and postsynaptic activity. *Journal of the Association for Research in Otolaryngology*, **4**(1), 1–23.
- Kopp-Scheinflug, C., Tolnai, S., Malmierca, M. S., & Rübsamen, R. (2008). The medial nucleus of the trapezoid body: comparative physiology. *Neuroscience*, **154**(1), 160–170.
- Kushmerick, C., Renden, R., & Von Gersdorff, H. (2006). Physiological temperatures reduce the rate of vesicle pool depletion and short-term depression via an acceleration of vesicle recruitment. *Journal of Neuroscience*, **26**(5), 1366–1377.
- Kuwabara, N., DiCaprio, R. A., & Zook, J. M. (1991). Afferents to the medial nucleus of the trapezoid body and their collateral projections. *Journal of Comparative Neurology*, **314**(4), 684–706.
- Kuwabara, N., & Zook, J. M. (1991). Classification of the principal cells of the medial nucleus of the trapezoid body. *Journal of Comparative Neurology*, **314**(4), 707–720.
- Kuwabara, N., & Zook, J. M. (1992). Projections to the medial superior olive from the medial and lateral nuclei of the trapezoid body in rodents and bats. *Journal of Comparative Neurology*, **324**(4), 522–538.
- Liberman, M. C. (1988). Physiology of cochlear efferent and afferent neurons: Direct comparisons in the same animal. *Hearing Research*, **34**(2), 179–191.
- Liberman, M. C., & Brown, M. C. (1986). Physiology and anatomy of single olivocochlear neurons in the cat. *Hearing Research*, **24**(1), 17–36.
- Maison, S., Adams, J. C., & Liberman, M. C. (2003). Olivocochlear innervation in the mouse: Immunocytochemical maps, crossed versus uncrossed contributions, and transmitter colocalization. *Journal of Comparative Neurology*, **455**(3), 406–416.
- Maison, S., Usubuchi, H., & Liberman, M. C. (2013). Efferent feedback minimizes cochlear neuropathy from moderate noise exposure. *Journal of Neuroscience*, **33**(13), 5542–5552.
- Mochida, S. (2011). Activity-dependent regulation of synaptic vesicle exocytosis and presynaptic short-term plasticity. *Neuroscience Research*, **70**(1), 16–23.
- Mountain, D. C. (1980). Changes in endolymphatic potential and crossed olivocochlear bundle stimulation alter cochlear mechanics. *Science* (80-), **210**(4465), 71–72.
- Mulders, W., & Robertson, D. (2000). Evidence for direct cortical innervation of medial olivocochlear neurones in rats. *Hearing Research*, **144**(1–2), 65–72.
- Mulders, W., & Robertson, D. (2002). Inputs from the cochlea and the inferior colliculus converge on olivocochlear neurones. *Hearing Research*, **167**(1–2), 206–213.
- Mulders, W., Winter, I. M., & Robertson, D. (2002). Dual action of olivocochlear collaterals in the guinea pig cochlear nucleus. *Hearing Research*, **174**(1–2), 264–280.
- Müller, M., Goutman, J. D., Kochubey, O., & Schlegelberger, R. (2010). Interaction between facilitation and depression at a large CNS synapse reveals mechanisms of short-term plasticity. *Journal of Neuroscience*, **30**(6), 2007–2016.
- Neher, E., & Sakaba, T. (2008). Multiple roles of calcium ions in the regulation of neurotransmitter release. *Neuron*, **59**(6), 861–872.
- Oatman, L. C. (1976). Effects of visual attention on the intensity of auditory evoked potentials. *Experimental Neurology*, **51**(1), 41–53.
- Ota, Y., Oliver, D. L., & Dolan, D. F. (2004). Frequency-specific effects on cochlear responses during activation of the inferior colliculus in the guinea pig. *Journal of Neurophysiology*, **91**(5), 2185–2193.
- Paolini, G., FitzGerald, J. V., Burkitt, A. N., & Clark, G. M. (2001). Temporal processing from the auditory nerve to the medial nucleus of the trapezoid body in the rat. *Hearing Research*, **159**(1–2), 101–116.
- Pyott, S. J., & Rosenmund, C. (2002). The effects of temperature on vesicular supply and release in autaptic cultures of rat and mouse hippocampal neurons. *Journal of Physiology*, **539**(2), 523–535.
- Rajan, R. (1988). Effect of electrical stimulation of the crossed olivocochlear bundle on temporary threshold shifts in auditory sensitivity. I. Dependence on electrical stimulation parameters. *Journal of Neurophysiology*, **60**(2), 549–568.
- Rajan, R. (1995). Frequency and loss dependence of the protective effects of the olivocochlear pathways in cats. *Journal of Neurophysiology*, **74**(2), 598–615.
- Ramón y Cajal, S. (1909). In A. Maloigne, (ed.), *Histologie du système nerveux de l'homme & des vertébrés*. Maloigne.
- Regehr, W. G. (2012). Short-term presynaptic plasticity. In: M Sheng, B Sabatini, & TCS (eds.), *Cold Spring Harbor perspectives in biology: The synapse* (pp 1–19). Cold Spring Harbor Laboratory Press.
- Reiter, E. R., & Liberman, M. C. (1995). Efferent-mediated protection from acoustic overexposure: Relation to slow effects of olivocochlear stimulation. *Journal of Neurophysiology*, **73**(2), 506–514.
- Robertson, D. (1984). Horseradish peroxidase injection of physiologically characterized afferent and efferent neurones in the guinea pig spiral ganglion. *Hearing Research*, **15**(2), 113–121.
- Robertson, D., & Gummer, M. (1985). Physiological and morphological characterization of efferent neurones in the guinea pig cochlea. *Hearing Research*, **20**(1), 63–77.
- Romero, G. E., & Trussell, L. O. (2021). Distinct forms of synaptic plasticity during ascending vs descending control of medial olivocochlear efferent neurons. *Elife*, **10**.
- Sabatini, B. L., & Regehr, W. G. (1996). Timing of neurotransmission at fast synapses in the mammalian brain. *Nature*, **384**(6605), 170–172.

- Sakaba, T., Schneggenburger, R., & Neher, E. (2002). Estimation of quantal parameters at the calyx of Held synapse. *Neuroscience Research*, **44**(4), 343–356.
- Siegel, J. H., & Kim, D. O. (1982). Efferent neural control of cochlear mechanics? Olivocochlear bundle stimulation affects cochlear biomechanical nonlinearity. *Hearing Research*, **6**(2), 171–182.
- Smith, P. H., Joris, P. X., Carney, L. H., & Yin, T. C. (1991). Projections of physiologically characterized globular bushy cell axons from the cochlear nucleus of the cat. *Journal of Comparative Neurology*, **304**(3), 387–407.
- Smith, P. H., Joris, P. X., & Yin, T. C. (1998). Anatomy and physiology of principal cells of the medial nucleus of the trapezoid body (MNTB) of the cat. *Journal of Neurophysiology*, **79**(6), 3127–3142.
- Sommer, I., Lingenhöhl, K., & Friauf, E. (1993). Principal cells of the rat medial nucleus of the trapezoid body: an intracellular in vivo study of their physiology and morphology. *Experimental Brain Research*, **95**(2), 223–239.
- Spirou, G. A., Brownell, W. E., & Zidanic, M. (1990). Recordings from cat trapezoid body and HRP labeling of globular bushy cell axons. *Journal of Neurophysiology*, **63**(5), 1169–1190.
- Suthakar, K., & Ryugo, D. K. (2017). Descending projections from the inferior colliculus to medial olivocochlear efferents: Mice with normal hearing, early onset hearing loss, and congenital deafness. *Hearing Research*, **343**, 34–49.
- Taranda, J., Maison, S. F., Ballester, J., Katz, E., Savino, J., Vetter, D. E., Boulter, J., Liberman, M. C., Fuchs, P. A., & Elgoyhen, A. B. (2009). A point mutation in the hair cell nicotinic cholinergic receptor prolongs cochlear inhibition and enhances noise protection. *PLoS Biology*, **7**(1), e1000018.
- Taschenberger, H., & von Gersdorff, H. (2000). Fine-tuning an auditory synapse for speed and fidelity: Developmental changes in presynaptic waveform, EPSC kinetics, and synaptic plasticity. *Journal of Neuroscience*, **20**(24), 9162–9173.
- Terreros, G., Jorratt, P., Aedo, C., Elgoyhen, A. B., & Delano, P. H. (2016). Selective attention to visual stimuli using auditory distractors is altered in alpha-9 nicotinic receptor subunit knock-out mice. *Journal of Neuroscience*, **36**(27), 7198–7209.
- Thompson, A. M., & Thompson, G. C. (1993). Relationship of descending inferior colliculus projections to olivocochlear neurons. *Journal of Comparative Neurology*, **335**(3), 402–412.
- Tolnai, S., Englitz, B., Scholbach, J., Jost, J., & Rübsamen, R. (2009). Spike transmission delay at the calyx of Held in vivo: Rate dependence, phenomenological modeling, and relevance for sound localization. *Journal of Neurophysiology*, **102**(2), 1206–1217.
- Tong, H., Kopp-Scheinflug, C., Pilati, N., Robinson, S. W., Sinclair, J. L., Steinert, J. R., Barnes-Davies, M., Allfree, R., Grubb, B. D., Young, S. M., & Forsythe, I. D. (2013). Protection from noise-induced hearing loss by kv2.2 potassium currents in the central medial olivocochlear system. *Journal of Neuroscience*, **33**(21), 9113–9121.
- Torres Cadenas, L., Fischl, M. J., & Weisz, C. J. C. (2020). Synaptic inhibition of medial olivocochlear efferent neurons by neurons of the medial nucleus of the trapezoid body. *Journal of Neuroscience*, **40**(3), 509–525.
- Van Hook, M. J. (2020). Temperature effects on synaptic transmission and neuronal function in the visual thalamus. *PLoS One*, **15**(4), 1–21.
- Vetter, D. E., Saldaña, E., & Mugnaini, E. (1993). Input from the inferior colliculus to medial olivocochlear neurons in the rat: A double label study with PHA-L and cholera toxin. *Hearing Research*, **70**(2), 173–186.
- Volgushev, M., Kudryashov, I., Chistiakova, M., Mukovski, M., Niesmann, J., & Eysel, U. T. (2004). Probability of transmitter release at neocortical synapses at different temperatures. *Journal of Neurophysiology*, **92**(1), 212–220.
- Wiederhold, M. L., & Kiang, N. Y. (1970). Effects of electric stimulation of the crossed olivocochlear bundle on single auditory-nerve fibers in the cat. *Journal of the Acoustical Society of America*, **48**(4B), 950–965.
- Wiederhold, M. L., & Peake, W. T. (1966). Efferent inhibition of auditory-nerve responses: Dependence on acoustic-stimulus parameters. *Journal of the Acoustical Society of America*, **40**(6), 1427–1430.
- Winslow, R. L., & Sachs, M. B. (1987). Effect of electrical stimulation of the crossed olivocochlear bundle on auditory nerve response to tones in noise. *Journal of Neurophysiology*, **57**(4), 1002–1021.
- Wu, S. H., & Kelly, J. B. (1993). Response of neurons in the lateral superior olive and medial nucleus of the trapezoid body to repetitive stimulation: Intracellular and extracellular recordings from mouse brain slice. *Hearing Research*, **68**, 189–201.
- Wu, S. H., Kelly, J. B., Shu Hui, W.U., & Kelly, J. B. (1993). Response of neurons in the lateral superior olive and medial nucleus of the trapezoid body to repetitive stimulation: Intracellular and extracellular recordings from mouse brain slice. *Hearing Research*, **68**, 189–201.
- Xie, R., & Manis, P. B. (2017). Radiate and planar multipolar neurons of the mouse anteroventral cochlear nucleus: Intrinsic excitability and characterization of their auditory nerve input. *Frontiers in Neural Circuits*, **11**, 1–17.
- Zhang, S., & Trussell, L. O. (1994). Voltage clamp analysis of excitatory synaptic transmission in the avian nucleus magnocellularis. *Journal of Physiology*, **480**(1), 123–136.
- Zucker, R. S., & Regehr, W. G. (2002). Short-term synaptic plasticity. *Annual Review of Physiology*, **64**(1), 355–405.

## Additional information

### Data availability statement

All data available upon reasonable request.

### Competing interests

None.



### Author contributions

All experiments were performed in the laboratory of C.J.C.W. C.J.C.W. conceived the study, C.J.C.W. and L.T. designed experiments, L.T. performed electrophysiological recordings, C.J.C.W., L.T. and H.C. analysed data and performed statistical analyses. C.J.C.W. wrote the paper with contributions from L.T. and H.C. All authors have read and approved the final version of this manuscript. All authors agree to be accountable for all aspects of the work in ensuring that questions related to the accuracy or integrity of any part of the work are appropriately investigated and resolved. All persons designated as authors qualify for authorship, and all those who qualify for authorship are listed.

### Funding

This research was supported by the Intramural Research Program of the NIH, NIDCD, Z01 DC000091 (C.J.C.W.).

### Keywords

auditory, efferent, inhibition, MNTB, MOC, olivocochlear

### Supporting information

Additional supporting information can be found online in the Supporting Information section at the end of the HTML view of the article. Supporting information files available:

### Peer Review History

### Statistical Summary Document